

# Acoustic limitations on the efficiency of machining by femtosecond laser-induced optical breakdown

Sanghyun Lee

Department of Mechanical Engineering, University of Michigan, Ann Arbor, Michigan 48109

Joseph L. Bull

Department of Biomedical Engineering, University of Michigan, Ann Arbor, Michigan 48109

Alan J. Hunt<sup>a)</sup>

Department of Biomedical Engineering, University of Michigan, Ann Arbor, Michigan 48109  
and Center for Ultrafast Optical Science, University of Michigan, Ann Arbor, Michigan 48109

(Received 14 February 2007; accepted 6 June 2007; published online 12 July 2007)

The authors find an unexpected strong influence of acoustic phenomena on the efficiency of water-assisted femtosecond laser nanomachining. Analysis of acoustic interactions across a metastable structure of two phase flow in a nanocapillary, predicts acoustic nodes that strongly limit machining efficiency. Strategies for fabrication of high aspect ratio channels ( $>1000$ ) are identified: increasing the speed of acoustic transmission delays formation of nodes, and can be accomplished by maximizing hydrogen in the gas phase or by varying pressure. These results reveal that laser machining can be strongly limited by acoustic phenomena not previously considered in the analysis of optical breakdown. © 2007 American Institute of Physics. [DOI: 10.1063/1.2752990]

Micrototal analysis systems ( $\mu$ TASs) endeavor to place complex analytic processes on a chip for simplified application, decreased costs, and minimal sample volumes. This requires complex micro- and nanofluidic networks to be integrated into a single chip, with increasing requirement for three-dimensional (3D) geometries and submicron scales, both of which are challenging to address through conventional two-dimensional planar lithography etch-bond processes. Laser-induced optical ablation by femtosecond laser pulses constitutes a promising method for submicron scale fabrication in dielectric materials,<sup>1-5</sup> and owing to the development of the water-assisted femtosecond laser machining,<sup>6,7</sup> it is now possible to directly fabricate true 3D nanochannels in the subsurface of dielectrics using far-field nanoablation,<sup>8-10</sup> without using a clean room, or challenging multilayer lithography processes.<sup>11</sup>

For femtosecond laser machining to reach its full potential for  $\mu$ TAS applications<sup>12</sup> requires production of high aspect ratio (AR) (=length/diameter) channels to realize complex 3D micro/nanofluidic networks. However, the AR has been limited to below 50 using laser or conventional drilling methods.<sup>13</sup> This limit can be overcome by taking advantage of the efficient extrusion of machining debris during water-assisted femtosecond laser machining.<sup>9</sup> However, at channel  $AR \approx 300$  machining becomes extremely slow and difficult: internal circulation due to expansion of bubbles produced by optical breakdown, which normally extrude machining debris, is severely attenuated as the bubbles become stationary. However, as the laser is scanned back and forth along an arc through and in front of the primary channel, a secondary channel forms visually discontinuous from the primary channel [Fig. 1(a)]; this discontinuity is taken to be the location of the first acoustic node. With further machining, the primary and secondary channels eventually unite, forming one

longer channel, as shown in Fig. 1(b). The machining rate in the discontinuity is very slow compared with that of the primary or secondary channel.

To produce high AR channels by femtosecond laser machining, water or other liquids are required to prevent accumulation of machining debris.<sup>6,9</sup> Debris entrained in the water is ejected from the channel by expanding bubbles, which move away from the ablation site and out the mouth of the channel, causing fluid circulation. Machining is expected to be limited as  $R_{cir}$  [Fig. 1(c)] rises to the point where debris extrusion is less than its generation; once this occurs, the machining rate will rapidly degrade with further increases in the channel length and  $R_{cir}$ . However, surprisingly diminished efficiency is localized; as shown in Fig. 1(c), once the

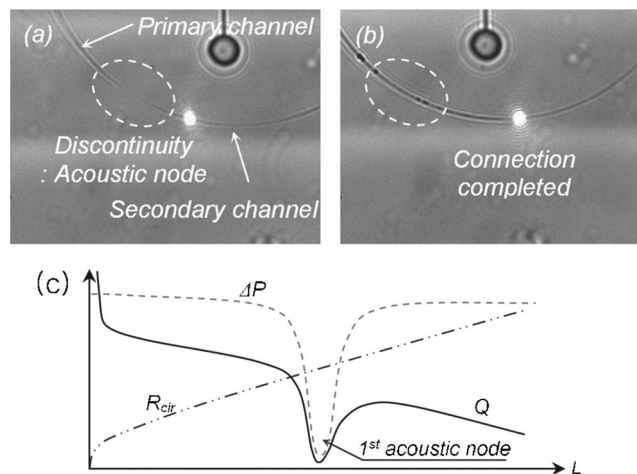


FIG. 1. (a) First acoustic node visually separates secondary and primary channels; (b) eventually they unite and form one longer channel. The water-assisted femtosecond laser nanomachining directly fabricate subsurface channels of  $\sim 600$  nm in diameter. (c) Schematics of retarded channel circulation due to the formation of an acoustic node which decreases the driving force  $\Delta P$  generated by bubble expansion. The circulation driving debris extrusion can be described by  $Q = \Delta P / R_{cir}$ , where  $R_{cir}$  is the resistance to circulation.

<sup>a)</sup> Author to whom correspondence should be addressed; electronic mail: ajhunt@umich.edu

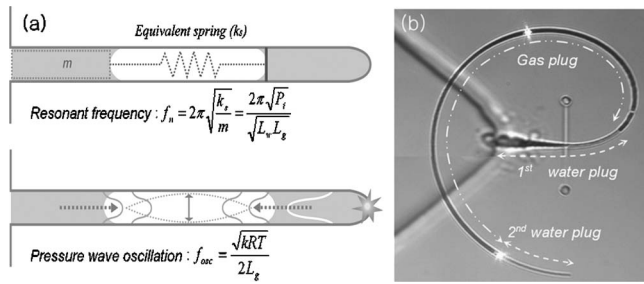


FIG. 2. (a) Analytic model for the first acoustic node. The gas plug acts as a spring and the water plug at the inlet port as a mass; the mass ( $m$ ) and equivalent spring constant ( $k_s$ ) following Boyle's law determine the  $f_n$ ;  $P_i$  is the internal pressure of the gas plug, and  $L_g$  and  $L_{w1}$  are the lengths of the gas and first water plugs. The  $f_{osc}$  in the gas plug is decided by the speed of sound and length of the gas plug;  $k$  is the specific heat ratio ( $c_p/c_v$ ),  $R$  is the gas constant, and  $T$  is the temperature of the gas plug. (b) Metastable WGW structure of the internal two phase flow; a large gas plug is formed in the middle of the channel, while the inlet and closed end of the channel are filled with water.

first local minimum of  $\Delta P$  is overcome machining efficiency is restored, until a second minimum is encountered at about twice the channel length. We hypothesize that this reflects the formation of acoustic nodes due to pressure cancellation in a metastable structure of two phase flow in a channel, analogous to the nodes in standing wave, though physically distinct.

Figure 2(b) shows a typical metastable structure of two phase flow during high AR channel machining. When the channel is short bubble expansion is vigorous, and no stable configurations form. However, at the initial site of inhibited machining (first node, see Fig. 1), a metastable water-gas-water (WGW) structure becomes evident.

If the resonance frequency ( $f_n$ ) of the WGW structure is matched to the pressure oscillation frequency ( $f_{osc}$ ) in the gas plug, the energy delivered to the ablation site may be readily transferred through the WGW structure, effectively canceling out bubble expansion at the ablation site. As shown in Fig. 2(a), two typical frequencies,  $f_n$  and  $f_{osc}$  are derived for the WGW structure. When the  $f_n$  and the  $f_{osc}$  are equal, the first acoustic node is formed.

$$f_{osc} = f_n \Rightarrow \frac{\sqrt{kRT}}{2L_g} = \frac{2\pi\sqrt{P_i}}{\sqrt{L_{w1}L_g}}. \quad (1)$$

The location of the first acoustic node is the total length of WGW structure ( $=L_{w1}+L_g+L_{w2}$ ); thus, the node equation is derived:

$$L_{node} \approx L_{w1} \left( 1 + \frac{k_{mix} R_{mix} T}{16\pi^2 (P_o + 160)} \right) + L_{w2}, \quad (2)$$

where  $k_{mix}$  and  $R_{mix}$  are the specific heat ratio and gas constant for the gas mixture, respectively. The temperature of gas plug is close to room temperature based on heat transfer analysis. The internal pressure  $P_i = P_o + 160$  kPa, which is elevated by capillary action, is experimentally determined

TABLE I. Gas composition of bubble by machining type; water was partially degassed by applying ultrasonic agitation under a vacuum.

| Machining type | Gas composition by mole fractions ( $0 \leq \alpha \leq 0.99$ )  |
|----------------|--|
| DWA, SWA       | $\alpha(\frac{2}{3}\text{H}_2 + \frac{1}{3}\text{O}_2) + (0.99 - \alpha)(0.65\text{N}_2 + 0.35\text{O}_2) + (0.01)\text{H}_2\text{O}(g)$ |
| Completely DWA | $0.99(\frac{2}{3}\text{H}_2 + \frac{1}{3}\text{O}_2) + (0.01)\text{H}_2\text{O}(g)$  |

from the compression of bubbles in the nanochannels when water is introduced,<sup>14</sup> this is consistent with less accurate estimates based on Laplace's law, which suffer from uncertainties in the contact angle and diameter of nanochannel.

To determine  $k_{mix}$  and  $R_{mix}$ , as shown in Table I, three possible sources are considered: (1) the dissociation of water molecules into hydrogen and oxygen, (2) diffusion of dissolved gases in water such as nitrogen and oxygen, and (3) water vapor; the maximum mole fraction of water vapor is approximately 1% at room temperature. Following the node equation, acoustic node formation is not directly dependent on laser parameters such as pulse energy and repetition rate. Experimentally pulse energy is found to change the node locations, however, does not appreciably change the AR of node location, considering the diameter of capillary also changes accordingly. However, at much higher repetition rates (100–200 kHz) preliminary results indicate that machining efficiency is severely limited due to complete dehydration of the channels; studies are ongoing to examine this in detail. The WGW structure and nodes can potentially form whenever the maximum bubble diameter is sufficient to occlude a channel or space during machining. Under our experimental conditions this limits the phenomena to machining scales below  $\sim 10 \mu\text{m}$ , but it may be significant at larger scales with higher pulse energies and larger bubbles.

The node equation is applied to and compared with the three experiments: two degassed-water-assisted (DWA) and one saturated-water-assisted (SWA) machinings. Using SWA the node forms at  $181 \mu\text{m}$ , and using  $\alpha=0.22$  the node equation gives exact agreement to the experiment. For the DWA experiments, the nodes occur at  $320$  and  $352 \mu\text{m}$ , which the node equation exactly predicts for  $\alpha=0.63$ ; for completely degassed water ( $\alpha=0.99$ ),  $413$  and  $458 \mu\text{m}$  are predicted as theoretical maxima. This is in good agreement considering that the water cannot be completely degassed in practice. As shown in Table II, by increasing the mole fraction of  $\text{H}_2$  degassing the water raises the speed of sound ( $\text{H}_2 \sim 1320$  m/s,  $\text{N}_2 \sim 350$  m/s, and  $\text{O}_2 \sim 330$  m/s) in gas plug, increasing the resonant length of the gas plug; thus the node formation is significantly delayed or inhibited.

The node equation also predicts that the node formation is controlled by the pressure  $P_o$ . As shown in Fig. 3, variation of  $P_o$  changes the location of the nodes, confirming accuracy and validity of the node equation. Using a custom built pressure controller to vary pressure from 90 to 130 kPa, the experiments follow the analytic predictions of the node equation.

TABLE II. Gas composition of bubbles predicted from the node position.

| Machining | $T$ (K) | $P_i$ (kPa) | $\text{H}_2$ | $\text{N}_2$ | $\text{O}_2$ | $\text{H}_2\text{O}(g)$ | $\alpha$ |
|-----------|---------|-------------|--------------|--------------|--------------|-------------------------|----------|
| DWA       | 295     | 260         | 0.42         | 0.234        | 0.336        | 0.01                    | 0.63     |
| SWA       | 295     | 260         | 0.147        | 0.501        | 0.343        | 0.01                    | 0.22     |

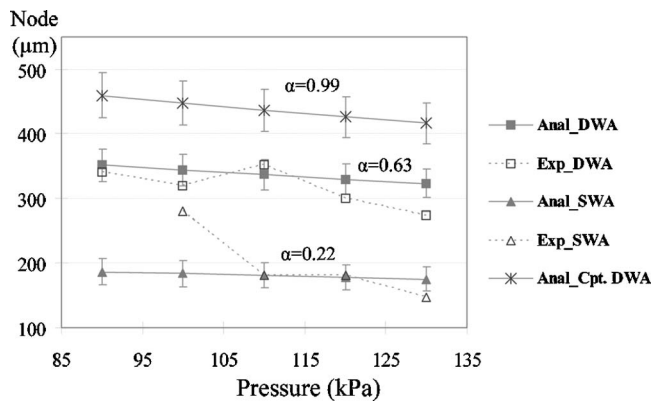


FIG. 3. Effect of pressure on the first acoustic node formation. To vary the pressure, a dc motor driven syringe pump was feedback controlled within 1%.

We have characterized a strong, previously unrecognized role of acoustic phenomena during femtosecond laser machining. Experiments and theory allow us to identify methods for machining high AR channels, which are critical for developing complex laboratory-on-a-chip and micrototal analysis devices. The submicron ( $\sim 600$  nm) diameter channels present significant advantages for producing complex devices in restricted spaces,<sup>9</sup> and for analytical methods such as capillary electrophoresis (CE), where reduced diameter allows increased separation rates with much smaller sample volume. However, to take full advantage of small, 3D channels sufficient length is also required: for example, CE requires high AR for good resolution.

Understanding the role of acoustics during femtosecond laser machining, thus, provides the basis to realize complex micro/nanofluidics with freedom to arbitrarily configure components in three dimensions. It also reveals the importance of parameters not generally considered in analyses of optical breakdown, and laser machining, such as the pres-

sure, gas composition, and resonant structures.

The authors are grateful to Edgar Meyhöfer and E. F. (Charlie) Hasselbrink for useful discussions. The authors thank IMRA Corp. and Intralase Corp. for use of lasers. This work was supported by a grant from IMRA Corp. and NIH R21 EB006098-01.

- <sup>1</sup>Ajit P. Joglekar, Hsiao-hua Liu, Edgar Meyhöfer, Gerard Mourou, and Alan J. Hunt, Proc. Natl. Acad. Sci. U.S.A. **101**, 5856 (2004).
- <sup>2</sup>Ajit J. Joglekar, Hsiao-hua Liu, Edgar Meyhöfer, Gerard Mourou, and Alan J. Hunt, Appl. Phys. B: Lasers Opt. **77**, 25 (2003).
- <sup>3</sup>A. Vogel, J. Noack, G. Hüttman, and G. Paltauf, Appl. Phys. B: Lasers Opt. **81**, 1015 (2005).
- <sup>4</sup>Joel P. McDonald, Vanita R. Mistry, Katherine E. Ray, and Steven M. Yalisove, Appl. Phys. Lett. **88**, 183113 (2006).
- <sup>5</sup>Chris B. Schaffer, André Brodeur, José F. García, and Eric Mazur, Opt. Lett. **26**, 93 (2001).
- <sup>6</sup>Yan Li, Kazuyoshi Itoh, Wataru Watanabe, Kazuhiro Yamada, Daisuke Kuroda, Junji Nishii, and Yongyuan Jiang, Opt. Lett. **26**, 1912 (2001).
- <sup>7</sup>R. An, Y. Li, Y. Dou, D. Liu, H. Yang, and Q. Gong, Appl. Phys. A: Mater. Sci. Process. **83**, 27 (2006).
- <sup>8</sup>Tyson N. Kim, Kyle Campbell, Alex Groisman, David Kleinfeld, and Chris B. Schaffer, Appl. Phys. Lett. **86**, 201106 (2005).
- <sup>9</sup>K. Ke, E. F. Hasselbrink, and Alan J. Hunt, Anal. Chem. **77**, 5083 (2005).
- <sup>10</sup>Sanghyun Lee, Alan J. Hunt, and E. F. Hasselbrink, Proceedings of the MicroTAS 2005 Conference, Boston, MA (Transducer Research Foundation, San Diego, 2005), Vol. 1, pp. 524–526.
- <sup>11</sup>Todd Thorsen, Sebastian J. Maerke, and Stephen R. Quake, Science **298**, 580 (2002).
- <sup>12</sup>P. S. Dittrich, K. Tachikawa, and A. Manz, Anal. Chem. **78**, 3887 (2006).
- <sup>13</sup>D. J. Hwang, T. Y. Choi, and C. P. Grigoropoulos, Appl. Phys. A: Mater. Sci. Process. **79**, 605 (2004).
- <sup>14</sup>See EPAPS Document No. E-APPLAB-90-096726 for a description on how to experimentally measure an internal pressure of bubbles/gas-plugs formed in nano-capillaries. Clearer and more straightforward methods of measuring the volume compression ratio than a theoretical expectation by Laplace's law allow to have empirical relation of internal pressure of nanobubbles, which gives a very solid basis in calculating node equation found in this research. This document can be reached via a direct link in the online article's HTML reference section or via the EPAPS homepage (<http://www.aip.org/pubservs/epaps.html>).